Environmental Fluctuations and Acoustic Data Communications

W.S. Hodgkiss and H.C. Song
Marine Physical Laboratory
Scripps Institution of Oceanography
La Jolla, CA 92093-0701
phone: (858) 534-1798/0954 / fax: (858) 822-0665
email: whodgkiss@ucsd.edu / hcsong@ucsd.edu

Award Number: N00014-11-1-0364
http://www.mpl.ucsd.edu

LONG-TERM GOALS

Couple together analytical and numerical modeling of oceanographic and surface wave processes, acoustic propagation modeling, statistical descriptions of the waveguide impulse response between multiple sources and receivers, and the design and performance characterization of underwater acoustic digital data communication systems in shallow water.

OBJECTIVES

Develop analytical/numerical models, validated with experimental data, that relate short-term oceanographic variability and source/receiver motion to fluctuations in the waveguide acoustic impulse response between multiple sources and receivers along with new communication receiver algorithms that exploit these channel characterizations.

APPROACH

The focus of this research is on how to incorporate an understanding of short-term variability in the oceanographic environment and source/receiver motion into the design and performance characterization of underwater acoustic, diversity-exploiting, digital data communication systems. The underlying physics must relate the impact of a fluctuating oceanographic environment and source/receiver motion to fluctuations in the waveguide acoustic impulse response between multiple sources and receivers and ultimately to the design and performance characterization of underwater acoustic digital data communication systems in shallow water.

The two major thrusts of this work include participation in a shallow water acoustic communication experiment in June-July 2011 along with subsequent analysis of the experiment data.

KAM11 Experiment (2011)

A shallow water acoustic communications experiment (KAM11) was carried out in June-July 2011 off the western side of Kauai, Hawaii at the Pacific Missile Range Facility (PMRF). Both fixed and towed source transmissions were carried out to multiple receiving arrays over ranges of approximately 1-14 km. Substantial environmental data was collected including water column sound speed structure

(CTDs and thermistor strings), sea surface directional wave field (waverider buoy), and local wind speed and direction. The focus was on fluctuations over scales of a few seconds to a few tens of seconds that directly affect reception of a data packet and packet-to-packet variability.

Algorithm Design and Experiment Data Analysis

Communication receiver algorithm design for shallow water is challenging due to the likelihood of encountering highly dynamic environments. In fact, one of the reasons for the KAM11 site selection was the variability of the environmental conditions (both sea surface and water column) from fairly calm to highly fluctuating. One emphasis of our work is mitigating Doppler and Doppler spread (both due to source-receiver motion as well as a fluctuating sea surface). Another emphasis of our work is multi-user receiver design in the presence of unsynchronized users (to accommodate networked communication). Lastly, a third emphasis of our work is communication algorithm design for very low signal-to-noise ratio (SNR) operations.

WORK COMPLETED

A shallow water acoustic communications experiment (KAM11) was conducted in early summer 2011 off the western side of Kauai, Hawaii [8]. Both fixed and towed source transmissions were carried out to multiple receiving arrays over ranges of 1-8 km along with additional towed source transmissions out to 14 km range. The acoustic transmissions were in three bands covering 3.5 to 35 kHz. Substantial environmental data was collected including water column sound speed structure (CTDs and thermistor strings), sea surface directional wave field (waverider buoy), and local wind speed and direction. The focus was on fluctuations over scales of a few seconds to a few tens of seconds that directly affect the reception of a data packet and packet-to-packet variability. The experiment region exhibited substantial daily oceanographic variability.

Analysis of the KAM11 experiment data this past year has focused on fixed source transmissions. Specifically, data investigating the influence of surface interacting ray paths was analyzed.

Publications related to this research involving analysis of KAM11 (and previous KAM08) data include [1-18].

RESULTS

During KAM11, two fixed source and vertical receive array systems were deployed near the seafloor by the University of Delaware [8]. These systems were ~1 km apart in ~100-108 m deep water (denoted Sta05 and Sta07 in Fig. 1). A hydrophone receiver monitoring the source transmissions was suspended from the R/V Kilo Moana approximately mid-way between the seafloor systems. The transmissions were 48 ms duration, 7-13 kHz, linear frequency modulated (LFM) chirps that were transmitted repeatedly every 144 ms for 40 s. The two sources alternated transmitting every 2 min for an extended period of time. Examples of the time-varying channel impulse response (CIR) from each source to the monitor hydrophone are shown in Figs. 1(b) (July 10, 2200 UTC) and 1(c) (July 10, 2206 UTC) [13]. The two vertical lines represent the direct and bottom bounce arrivals. The time-varying arrivals that follow in pairs correspond to the surface bounce and the bottom-surface bounce. Note the emergence of scattered, slanted later arrivals that collectively generate a striation pattern in the tail. These patterns run in opposite directions for the two sources. In this case, the dominant surface wave direction was from the NE and roughly aligned with the two sources and monitor hydrophone.

A ray tracing algorithm capable of treating a traveling surface wave field can be employed to simulate the time-varying CIR caused by a dynamic sea surface [13]. Both ray travel time and amplitude are computed as the point of intersection with the sea surface follows continuously along the surface resulting in the observed striation pattern. A simplified example consisting of a sinusoidal sea surface with ideal half-space below (1500 m/s sound speed) will illustrate the concept [13]. Both the source and receiver are positioned at 10 m below the mean surface as shown in Fig. 2(a). The horizontal separation of 200 m contains 5 full wave cycles. The simulated time-varying CIR using the ray tracing model is shown in Figs. 2(b) and 2(c) when the surface wave is traveling from left-to-right (forward) and from right-to-left (backward), respectively. The CIR is computed every 50 ms for a 20 s period. The first vertical line at 133.3 ms is the direct horizontal arrival. The second vertical line near 134 ms is the surface bounce from the vicinity of the specular reflection point in the middle (i.e. 100 m). Specifically, the shortest surface bounce path occurs during the passage of a trough near midrange. Note the emergence of a curved striation pattern in both directions immediately following the surface reflected arrival, extended over 1 ms upward (advancing arrivals) and downward (retreating arrivals). The symmetric striation pattern is due to the simplified geometry simulated. An asymmetric source-receiver geometry results in a striation pattern that is dominated by upward or downward striations depending on direction of propagation of the surface waves [13].

The KAM11 environment now is simulated [13]. A realization of a random rough surface consistent with a concurrently measured surface wave spectrum is displayed in Fig. 3(a). The simulated time-varying CIR at the receiver is shown in Figs. 3(b) for Sta07 source (forward traveling surface wave) and Fig. 3(c) Sta05 source (backward traveling surface wave). The paths are numbered on top of the figure and correspond go (1) direct, (2) bottom bounce, (3) surface bounce, and (4) bottom-surface bounce. The modeling results in Fig. 3 can be compared to the experimental data in Fig. 1. While there are differences in detail, the simulation results appear to capture the essential features of the striation pattern seen in the experimental data. Specifically, the striation highlighted in the box emerges upward for the forward propagating surface wave (moving in the same direction as the source-receiver path) and downward for the backward propagating surface wave (moving in the opposite direction as the source-receiver path).

IMPACT / APPLICATIONS

Acoustic data communications is of broad interest for the retrieval of environmental data from in situ sensors, the exchange of data and control information between AUVs (autonomous undersea vehicles) and other off-board/distributed sensing systems and relay nodes (e.g. surface buoys), and submarine communications.

RELATED PROJECTS

In addition to other ONR Code 322OA and Code 321US projects investigating various aspects of acoustic data communications from both an ocean acoustics and signal processing perspective, two recently completed MURIs also focused on acoustic communications (W. Hodgkiss, “Impact of Oceanographic Variability on Acoustic Communications” and J. Preisig, “Underwater Acoustic Propagation and Communications: A Coupled Research Program”).

PUBLICATIONS

[1] S. Cho, H.C. Song, and W.S. Hodgkiss, "Successive interference cancellation for underwater acoustic communications," IEEE J. Oceanic Engr. 36(4): 490-501, DOI: 10.1109/JOE.2011.2158014 (2011). [published, refereed]

[2] H.C. Song, "Time reversal communication in a time-varying sparse channel," J. Acoust. Soc. Am. 130(4): EL161-EL166, DOI: 10.1121/1.3629138 (2011). [published, refereed]

[3] Y. Isukapalli, H.C. Song, and W.S. Hodgkiss, "Stochastic channel simulator based on local scattering functions," J. Acoust. Soc. Am. 130(4): EL200-EL205, DOI: 10.1121/1.3633688 (2011). [published, refereed]

[4] T. Kang, H.C. Song, and W.S. Hodgkiss, "Multi-carrier synthetic aperture communication in shallow water: Experimental results," J. Acoust. Soc. Am. 130(6): 3797-3802, DOI: 10.1121/3652855 (2011). [published, refereed]

[5] S. Cho, H.C. Song, W.S. Hodgkiss, "Multiuser interference cancellation in time-varying channels," J. Acoust. Soc. Am. 131(2): EL163-EL169, DOI: 10.1121/1.3678668 (2012). [published, refereed]

[6] H.C. Song, "Bidirectional equalization for underwater acoustic communication," J. Acoust. Soc. Am. 131(4): EL343-EL347, DOI: 10.1121/1.3695075 (2012). [published, refereed]

[7] S. Cho, H.C. Song, and W.S. Hodgkiss, "Asynchronous multiuser underwater acoustic communications (L)," J. Acoust. Soc. Am. 132(1): 5-8, DOI: 10.1121/1.4726029 (2012). [published, refereed]

[8] W.S. Hodgkiss and J.C. Preisig, "Kauai Acomms MURI 2011 (KAM11) Experiment," Proc. 11th European Conference on Underwater Acoustics (ECUA): 1-8 (2012). [published]

[9] S. Cho, H.C. Song, and W.S. Hodgkiss, "Multiuser acoustic communications with mobile users," J. Acoust. Soc. Am. 133(2): 880-890, DOI: 10.1121/1.4773267 (2013). [published, refereed]

[10] H.C. Song and W.S. Hodgkiss, "Efficient use of bandwidth for underwater acoustic communication (L)," J. Acoust. Soc. Am. 134(2): 905-908, DOI: 10.1121/1.4812762 (2013). [published, refereed]

[11] W.S. Hodgkiss, H.C. Song, and D.E. Ensberg, "Wideband channel impulse response fluctuations in shallow water," Proc. 1st Intl. Conf. Underwater Acoustics (UA) 2013: 1565-1570, ISBN 978-618-80725-0-3 (2013). [published]

[12] H.C. Song, "Equivalence of adaptive time reversal and least squares for cross talk mitigation," J. Acoust. Soc. Am. 135(3): EL154-EL158, DOI: 10.1121/1.4865839 (2014). [published, refereed]

[13] Y. Choo, W. Seong, and H.C. Song, "Emergence of striation patterns in acoustic signals reflected from dynamic surface waves," J. Acoust. Soc. Am. 136(3): 1046-1053, DOI: 10.1121/1.4892765 (2014). [published, refereed]

[14] W.S. Hodgkiss, H.C. Song, and D.E. Ensberg, "Statistical characterization of wideband channel impulse response observations in shallow water," Proc. 2nd Intl. Conf. Underwater Acoustics (UA2014): 1535-1540, ISBN: 978-618-80725-1-0 (2014). [published]

[15] H.C. Song and W.S. Hodgkiss, "Self-synchronization and spatial diversity of passive time reversal communication (L)," J. Acoust. Soc. Am. 137(5): 2974-2977, DOI: 10.1121/1.4919324 (2015). [published, refereed]

[16] H.C. Song and C. Cho, "The relation between the waveguide invariant and the array invariant," J. Acoust. Soc. Am. 138(2): 899-903, DOI: 10.1121/1.4927090 (2015). [published, refereed]

[17] H.C. Song, "An overview of underwater time-reversal communications," IEEE J. Oceanic. Engr., DOI: 10.1109/JOE.2015.2461712 (2015). [in press, refereed]

[18] R. Otnes, P.A. van Walree, H. Buen, and H.C. Song, "Underwater acoustic network simulation with lookup tables from physical-layer replay," IEEE J. Oceanic. Engr. 40(4): 822-840, DOI: 10.1109/JOE.2015.2471736 (2015). [published, refereed]

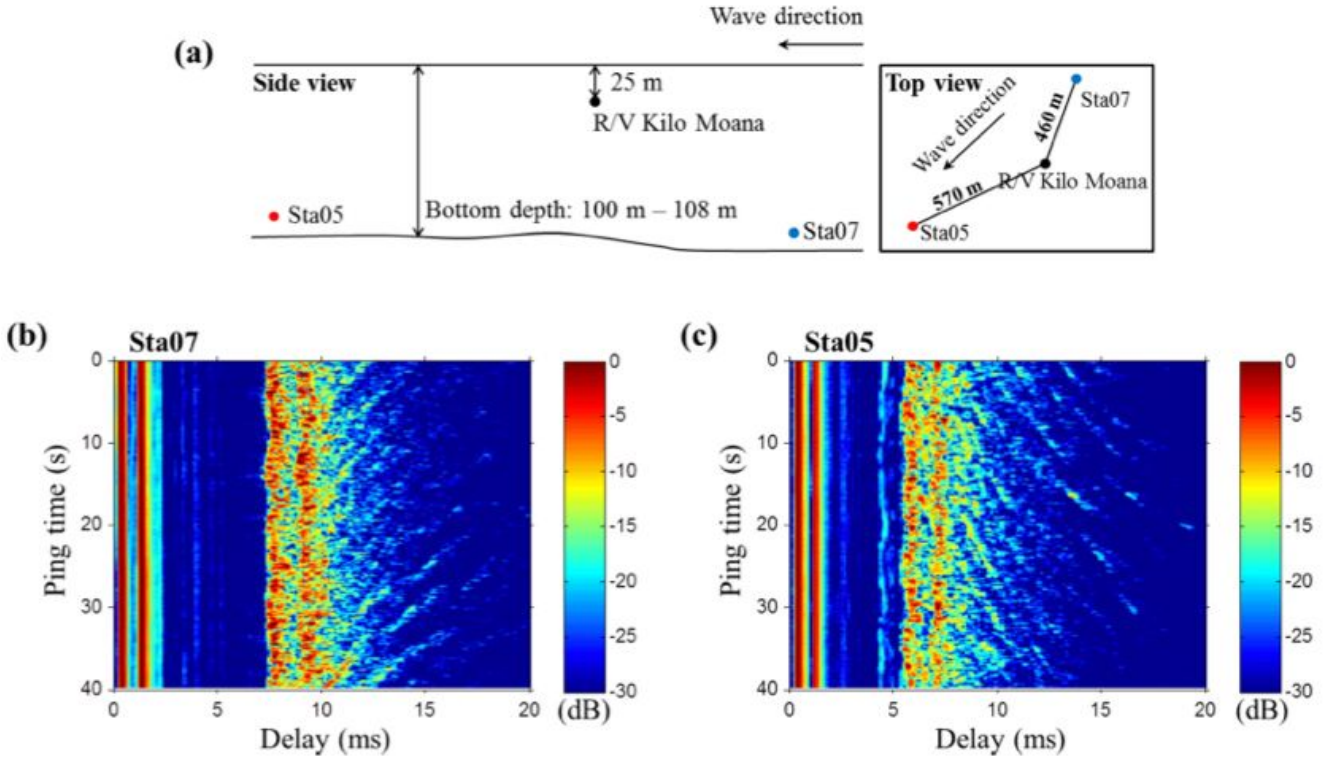

Figure 1. (a) Schematic of the KAM1 experiment along with a top view of the source-receiver geometry and dominant surface wave direction (NE to SW). Two sources located at Sta05 and Sta07 were moored 2 m above the seafloor and a monitoring hydrophone was suspended from the R/V Kilo Moana at 25 m depth. (b) Channel impulse response from the Sta07 source (July 10, 2200 UTC). (c) Channel impulse response from the Sta05 source (July 10, 2206 UTC). The horizontal axis is relative delay and the vertical axis is ping time. The two vertical lines represent the direct and bottom bounce arrivals. The time-varying arrivals followed in pairs and correspond to the surface bounce and the bottom-surface bounce. Note that a striation pattern in (b) and (c) emerges in opposite directions in the tail.

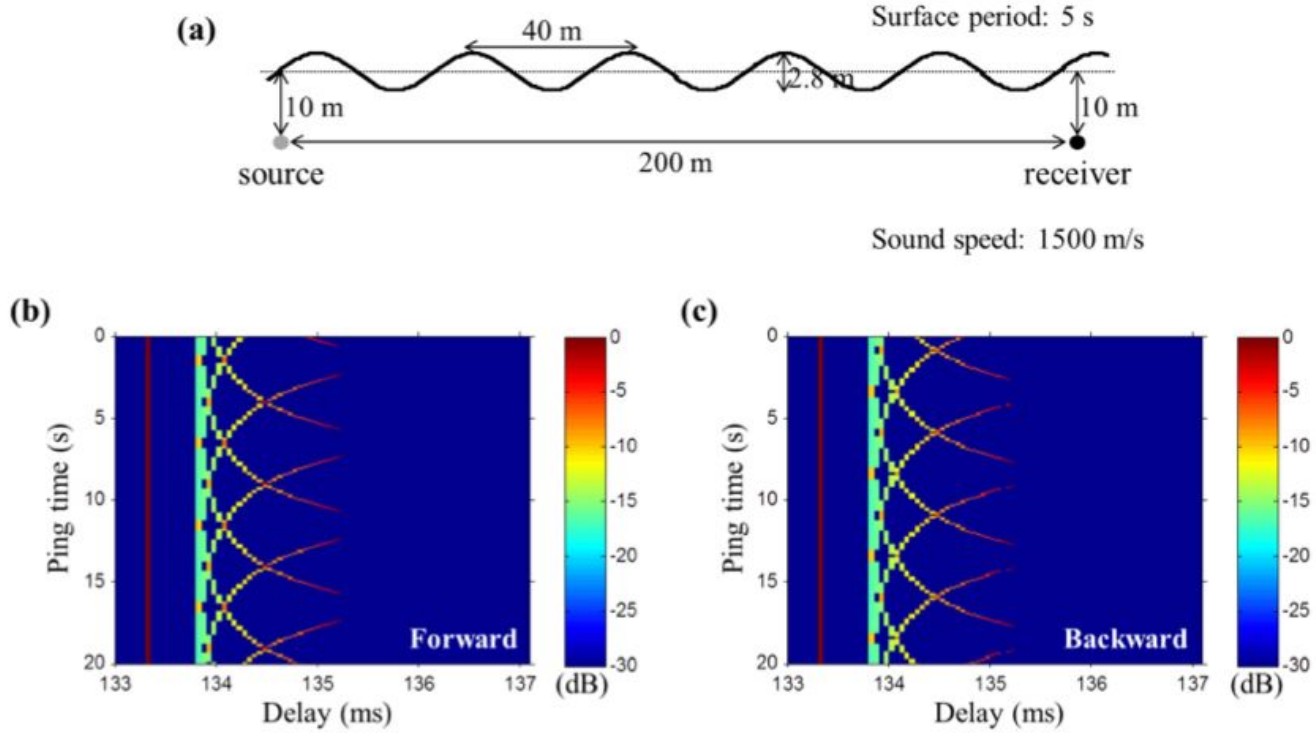

Figure 2. Simulation results for a sinusoidal surface and a symmetric source-receiver geometry in an ideal half-space. (a) The surface wave frequency is 0.2 Hz with a wavelength of 40 m and the wave height of 2.8 m peak-to-trough. The sound speed is 1500 m/s. The source and receiver both are at 10 m below the mean sea surface and separated by 200 m. (b) Modeled channel impulse response when the surface wave is moving from left-to-right (forward), in the same direction as acoustic propagation. (c) Modeled channel impulse response when the surface wave is moving from right-to-left (backward), in the opposite direction of acoustic propagation. The striation pattern emerges in both directions (upward and downward) and is symmetric regardless of the surface wave direction.

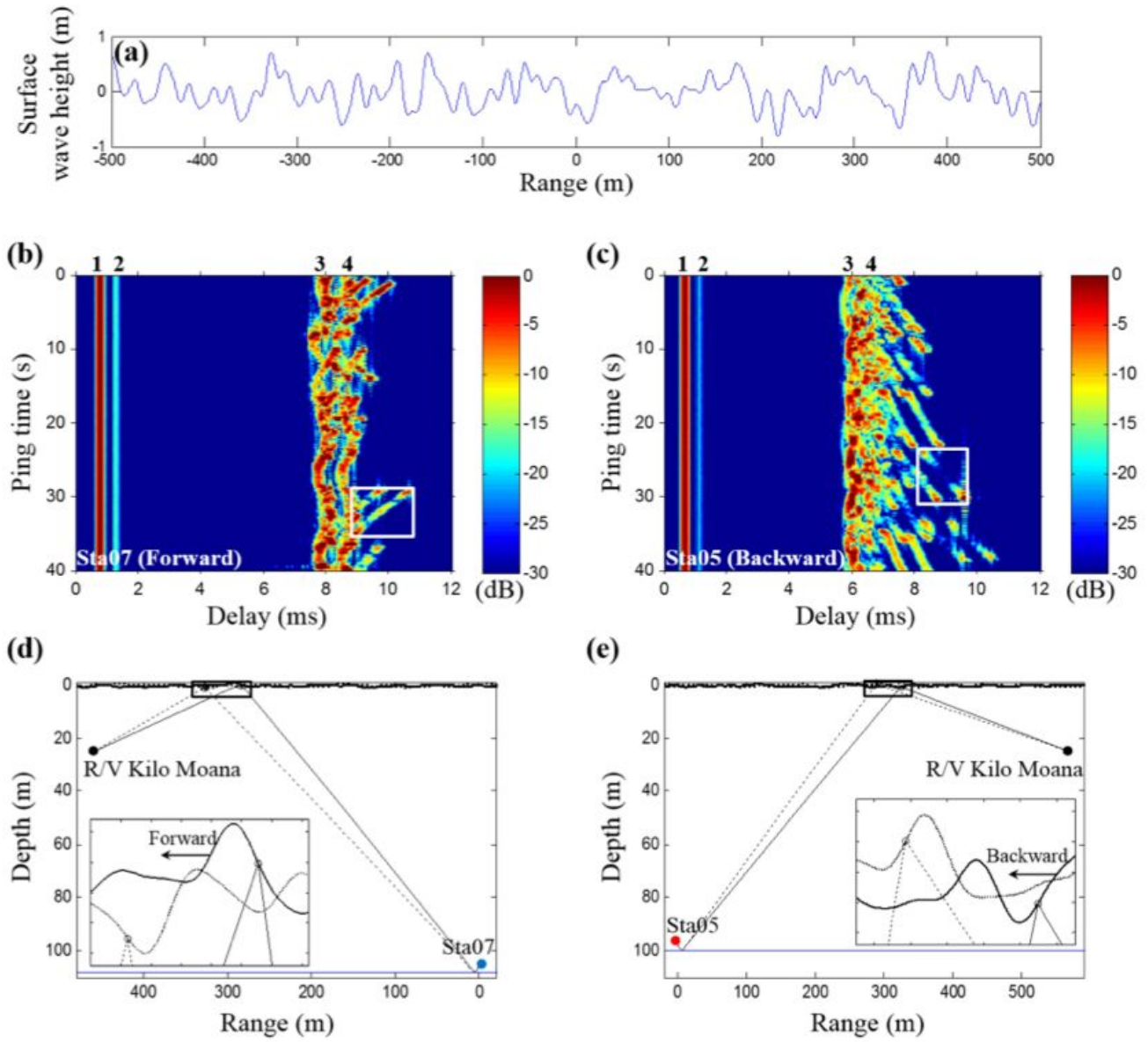

Figure 3. Broadband simulation corresponding to the KAM11 experiment displayed in Fig. 1. (a) Realization of a smooth surface wave profile based on the measured directional wave spectrum. The surface wave is assumed to travel from right-to-left. (b) Modeled channel impulse response from the Sta07 source. (c) Modeled channel impulse response from the Sta05 source. Panels (d) and (e) both show the region of illumination and close-up view of rays interacting with the irregular surface, corresponding to panels (b) and (c), respectively.